Brillouin light scattering from poly(methyl methacrylate)/toluene concentrated solutions

ARTICLE *in* MACROMOLECULES · MARCH 1992

Impact Factor: 5.8 · DOI: 10.1021/ma00028a046

Brillouin Light Scattering from Poly(methyl methacrylate)/Toluene Concentrated Solutions

Wyn Brown,* Karin Schillén, and Robert Johnsen

Institute of Physical Chemistry, University of Uppsala, Box 532, 751 21 Uppsala, Sweden

Cestmir Konak and Ladislav Dvoranek

Institute of Macromolecular Chemistry, Czechoslovak Academy of Sciences, 162 06 Prague 6, Czechoslovakia

Received February 13, 1991; Revised Manuscript Received October 21, 1991

ABSTRACT: A Brillouin scattering study of poly(methyl methacrylate)/toluene mixtures at various polymer concentrations and temperatures has been carried out. The temperature dependences of the Brillouin shifts and line widths are qualitatively explained in terms of the relaxation time model. The concentration dependences of the Brillouin data are discussed in light of a theory for Brillouin light scattering from gels proposed by Marqusee and Deutch (M&D). The speed of sound in the network and frictional damping have been evaluated from the Brillouin shifts and line widths, respectively. Although it provides a realistic description of the data at the lower concentrations, the M&D theory breaks down in the vicinity of the line-width maximum, giving values of the frictional coefficient which are too small in this region.

Introduction

Rayleigh–Brillouin scattering is an important tool for probing relaxation processes in molecular fluids, including polymer fluids. This spectroscopic method has been widely used, for example, in studies of mechanical relaxation in bulk polymers at high frequencies (e.g., refs 1 and 2). While concerted efforts have been made to improve understanding of the dynamical properties of solutions and gels using quasielastic light scattering (e.g., refs 3–5), comparatively little attention has been focused on Brillouin scattering in binary polymer/solvent systems (such as concentrated solutions and gels.[6-13] In the latter case, density fluctuations propagating through the medium as hypersound waves suffer additional scattering from the relatively fixed elastic polymer network. This scattering leads to a shorter lifetime for density fluctuations and hence to spectral broadening. Conversely, the shift and width of the Brillouin light scattering peaks could be suitably employed to investigate the static and dynamical properies of concentrated polymer solutions and gels. The purpose of this work is to check this possibility.

Concentrated solutions of poly(methyl methacrylate) (PMMA) in toluene have been investigated by Brillouin light scattering spectroscopy (BLSS) over a broad concentration range extending up to the bulk. A particular difficulty can be the overriding part contributed by concentration fluctuations to the scattered light and the consequent difficulty in making a precise determination of the density fluctuations. The present system was selected since toluene is almost isorefractive with PMMA, and thus the contribution of concentration fluctuations to the scattered light is strongly reduced. New and original data on the static and dynamic behavior of concentrated PMMA solutions have been obtained. A good theoretical description of Brillouin scattering from solutions is not yet available. The approach taken here is to utilize the existing framework developed by Marqusee and Deutch for gels.[14] It will be shown that serious deficiencies exist when it is applied to the data for polymer solutions.

Experimental Section

Sample Preparation. The polymerization inhibitor was removed by rinsing the methyl methacrylate (MMA) with an alkaline solution. The monomer was washed with distilled water, dried with sodium sulfate and calcium hydride, and distilled in a column under reduced pressure in a stream of nitrogen.

The mixture of MMA with carefully distilled toluene and di-*tert*-butyl peroxide (1×10^{-2} M with respect to the monomer) was dosed into the stock ampule of a dust-free polymerization apparatus and degassed by several freeze–thaw cycles. The apparatus was then sealed. Dust was removed from the mixture of monomers by repeated slow freezing in the polymerization ampule, followed by decantation (checked by the absence of glitters in the He–Ne laser beam passing through the monomer). Finally, the cell containing the pure monomer mixture was sealed and placed in an oil bath. Polymerization was allowed to proceed at 120 °C for 36 h. On completion, the cell was slowly cooled (0.1 °C/min with a 24-h period at 100 °C) to prevent internal stresses in the polymer.

The conversion of the polymerization was about 95% at monomer volume fraction $\Phi = 0.1$ and increased with increasing concentration to almost 99% in the bulk sample. The weight-average molecular mass, M_w, of the poly(methyl methacrylate) samples is given for selected samples in Table I.

Brillouin Light Scattering Spectrometer. A block diagram of the optical system used for measuring quasielastic (Rayleigh) and Brillouin light scattering spectra is shown in Figure 1. The light source is an Ar ion laser (Coherent 304) which illuminates the sample cell through lens L_1 (focal length, $f_1 = 250$ mm). A single-mode laser beam with $\lambda = 488$ nm was employed. The scattered light may be analyzed in two ways:

(a) Both the quasielastic (QELS) and Brillouin spectra can be measured simultaneously. The QELS spectra are detected through diaphragm DP (0.5 mm in diameter), lens L_2 ($f_2 = 100$ mm), and the optical fiber F (0.1 mm in diameter) supported on the revolving arm, rendering possible measurements at scattering angles θ from 10 to 160°. The electronic beats from the photomultiplier PM_1 (EMI 9863B) are analyzed using a multi-τ autocorrelator (ALV-5000). The Brillouin light scattering measurements were performed at the fixed scattering angle $\theta = 90 \pm 0.1°$. The scattered light is collected through iris diaphragm I by the lens L_3 ($f_3 = 75$ mm) located at the focal distance from the scattering volume and focused by lens L_4 ($f_4 = 100$ mm) on the pinhole PH_1 (0.1 mm in diameter) located at the focal point of L_4. The parallel beam expanded by lens L_5 ($f_5 = 200$ mm) is passed through a piezoelectrically scanned three-pass Fabry–Perot interferometer (Tropel Model 350) and collimated by lens L_6 ($f_6 = 300$ mm) on the pinhole PH_2 (0.2 mm in diameter) and detected by the second photomultiplier PM_2 (Hamamatsu R464). The reflectivity and flatness figures defining the mirrors are 92% and $\lambda/200$, respectively. The actually realized finesse was in excess of 40, and the free spectral range of the Fabry–Perot interferometer was 36.6_1 GHz. The spectra are collected in a 1024-channel

0024-9297/92/2225-0802$03.00/0

Table I
Experimental Results Evaluated from the Fabry–Perot Spectra and Hypersound Speeds in Polymer Solutions and Polymer Networks

Φ	$M_w \times 10^3$	ν_B, GHz	$\Delta\nu_B$, MHz	c, m/s	c_n for $\lambda = 1$, m/s
0.0		6.00	510	1390	
0.1	100	6.02	530	1400	270
0.2	122	6.12	600	1420	430
0.3		6.17	670	1430	540
0.4		6.70	820	1550	790
0.5	345	7.49	990	1730	1090
0.6		8.52	970	1970	1440
0.7	590	10.38	570	2400	1980
0.8		11.18	340	2590	2220
0.9	420	12.06	160	2790	2500
1.0	54	12.49	150	2890	2890

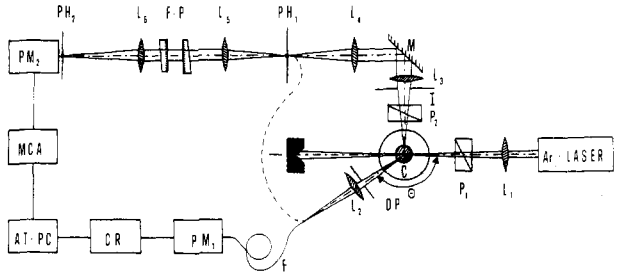

Figure 1. Block diagram of the instrument used: L_i (i = 1–6), lenses; C, sample cell; P_i (i = 1 and 2), polarizers; DP, diaphragm; PH_i (i = 1 and 2), pinholes; PM_i (i = 1 and 2), photomultipliers; I, iris diaphragm; F, optical fiber; θ, scattering angle; F–P, Fabry–Perot interferometer; MCA, multichannel analyzer; AT-PC, personal computer; CR, autocorrelator.

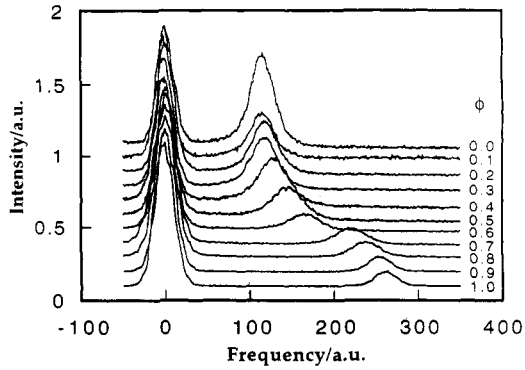

Figure 2. Fabry–Perot spectra of a series of poly(methyl methacrylate) samples with polymer volume fraction Φ_p = 0–1 as indicated (1 channel ≈ 50 MHz).

multichannel analyzer (MCA) using a scan time of 1 s and analyzed with an IBM AT personal computer.

(b) The angle dependence of Brillouin light scattering spectra can be measured. The output of the optical fiber is inserted in the front of the F–P interferometer instead of PH_1 (the dashed line). The diameter of DP must be increased to widen the viewing angle of the light detector.

Only polarized (VV) Rayleigh–Brillouin spectra are examined in this work. The data were analyzed by a nonlinear least-squares fitting procedure of Lorentzian functions based on the Marquardt algorithm,[15] as implemented in *Numerical Recipes*.[16] Assuming Poisson statistics, the squared residuals were weighted with the reciprocals of the measured values. The line width, $\Delta\nu_B$, was corrected for instrumental broadening by subtracting the instrumental half-width from the observed half-width at half-height. The experimental uncertainty was about 50 MHz for ν_B and ±25% for $\Delta\nu_B$ (run-to-run uncertainty).

Results

Figure 2 shows the Fabry–Perot spectra of a series of samples with starting monomer volume fraction Φ ranging from 0 to 1 at 25 °C. The spectra were collected in a 1024-channel multichannel analyzer using a scan time of

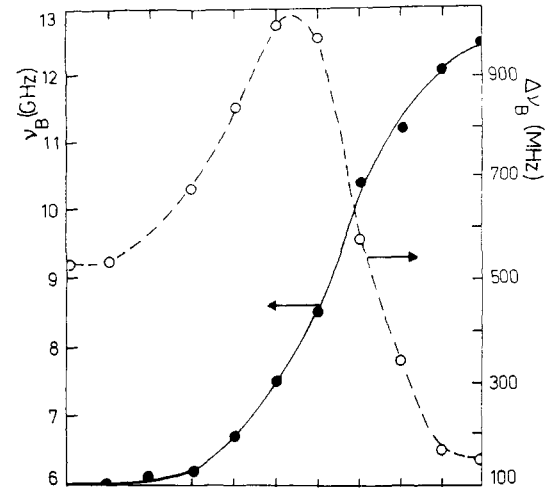

Figure 3. Line width $\Delta\nu_B$ of the Brillouin doublet and the Brillouin frequency shift ν_B plotted as a function of the volume fraction Φ_p.

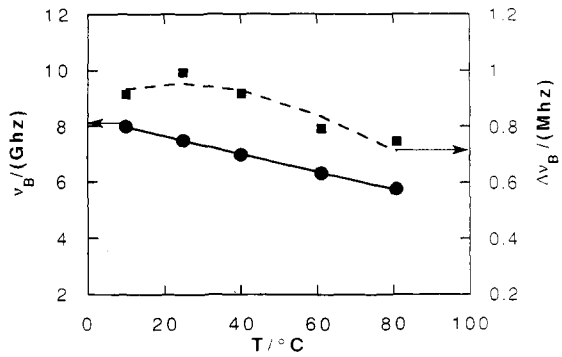

Figure 4. Temperature dependence of ν_B and $\Delta\nu_B$ for a sample with Φ_p = 0.5.

1 s and represent some 1000 scans of the spectrum. One may note that the spectrum is a sensitive function of solution fluidity and the viscosity changes greatly with Φ.

The line width $\Delta\nu_B$ of the Brillouin doublet and the Brillouin frequency shift ν_B evaluated from the spectra are shown in Figure 3 and collected in Table I as a function of Φ, including both pure polymer and the solvent. The line-width data presented in this paper correspond to the whole width at half-height. A nonlinear increase of the frequency ν_B with increasing concentration, as well as the existence of a line-width maximum at Φ = 0.5, is clearly evident. Furthermore, one notes that there is a change of slope in the curve of frequency ν_B versus Φ; the slope increases at the same volume fraction at which the maximum in $\Delta\nu_B$ is observed.

In order to examine the region of the hypersonic loss maximum, the temperature dependences of ν_B and $\Delta\nu_B$ were determined for the sample with Φ = 0.5 over the range 10–80 °C (see Figure 4). One sees in this figure that there is a line-width maximum in the frequency $\Delta\nu_B$ versus temperature (T) data at room temperature.

Discussion

Phonon Shift and Attenuation. At present there is no satisfactory theory which can be used to interpret the Brillouin spectrum of a polymer solution and/or gel.

The changes in ν_B and $\Delta\nu_B$ with concentration and temperature (Figures 3 and 4) are very similar to those observed earlier in polystyrene/cyclohexane solutions[9] and can be qualitatively explained in terms of the relaxation-time model.[1] Thus Figure 3 shows that the solvent and low-concentration solutions are in the low-frequency region where $\tau_S \ll 1/\nu_B$, while the polymer is either in or

approaching the high-frequency regime where $\tau_S \gg 1/\nu_B$. The line-width maximum occurs for a concentration at which $\tau_S \approx 1/\nu_B$. An analogous situation can be seen in Figure 4. The measurements at high temperatures were made below the relaxation region ($\tau_S \ll 1/\nu_B$), and low-temperature measurements were made above the range ($\tau_S \gg 1/\nu_B$).

In order to analyze the origin of the relaxation, detailed depolarized Rayleigh and polarized Rayleigh–Brillouin scattering measurements have also been made on the present samples and are presented elsewhere.[21] The polarized Rayleigh–Brillouin measurements revealed the presence of significant rotational mobility of the toluene, serving to initiate the broad hypersonic attenuation which is observed at gigahertz frequencies.

Since the relaxation-time model is limited to a phenomenological description only, we have sought an appropriate theory founded on a more advanced structural base. Such seems to be that described by Marqusee and Deutch,[14] dealing with Brillouin scattering from polymer gels. The physical picture adopted is similar to that describing flow in porous media. Their analysis includes coupling between the sound waves in the fluid and the elastic waves in the polymer network that is presented in the absence of any dissipative mechanisms. Marqusee and Deutch define a parameter $0 < \lambda < 1$, which is a measure of this coupling. Explicit expressions are given for the eigenmodes of the gel in the presence of both weak and strong frictional damping. Two-mode types of behavior are predicted in the former case. The latter limiting case essentially corresponds to a one-mode type of behavior and predicts a single pair of Brillouin peaks at $\pm\nu_B$. Since the measurements of the Brillouin spectra of the PMMA/toluene system reported here show the presence of only a single pair of Brillouin peaks, the theory in the limit of strong friction, f, has been adopted to analyze our results. The predictions of the theory for the average speed of sound in the medium c ($=2\pi\nu_B/q$) and width Γ ($=\Delta\nu_B\pi/q^2$) are[12,16]

$$c^2 = \frac{c_0^2\rho_f + \Phi_p(c_n^2\rho_n - c_0^2\rho_f) + 2c_0c_n[\lambda\rho_n\rho_f(\Phi_p - \Phi_p^2)]^{1/2}}{\rho_f + \Phi_p(\rho_n - \rho_f)} \quad (1)$$

$$2\Gamma = \frac{(4/3)\eta_s + \eta_B}{\rho_f + \Phi_p(\rho_n - \rho_f)} + \frac{\rho_f^2\rho_n^2(\Phi_p - \Phi_p^2)^2}{fc^2[\rho_f + \Phi_p(\rho_n - \rho_f)]^3} \times [c_0^2 - c_n^2 - c_0c_n(\rho_f - \Phi_p(\rho_n + \rho_f))(\lambda/\rho_n\rho_f(\Phi_p - \Phi_p^2))^{1/2}]^2 \quad (2)$$

where q is the wave vector of the sound, c_0 and c_n are the speeds of sound in the solvent and in the network, respectively, ρ_f and ρ_n are the corresponding densities of the fluid and solid phases, and Φ_p is the polymer volume fraction. $(4/3)\eta_s + \eta_B = 1/\rho_f\Gamma_0$, where Γ_0 is the width of the Brillouin line for the solvent (η_s and η_B are the hypersonic shear and bulk viscosities).

The parameter λ, the speed of sound in the network c_n, and the friction f are unknown functions of Φ_p. Originally, c_n was assumed to be only weakly dependent on Φ_p.[19] In comparison with experimental data, the prediction of the theory for ν_B (eq 1) calculated with $c_n = c(\Phi_p=1)$ provides an incorrect curvature of the ν_B versus Φ_p dependence.[12] In order to obtain a realistic description of the experimental data in terms of this theory, we have supposed in accordance with the conclusion in ref 12 that c_n and f are concentration-dependent, contrary to theoretical expectations. Such an assumption for c_n seems to be plausible since a higher concentration usually means an increased number of entanglements, which will tend to increase c_n.[17] As for the friction, f, its increase with increasing polymer concentration can be expected. The resulting prediction for $c_n(\Phi_p)$ can be obtained from eq 1. Physical constants required for calculations are listed in Table II. The value of $(4/3)\eta_s + \eta_B$ was calculated from the line width of toluene given in Table I. The results of the $c_n(\Phi_p)$ calculation are shown in Figure 5 and Table I for $\lambda = 0, 0.25, 0.5, 0.75$, and 1, using the physical constants in Table II. The polymer volume fraction Φ_p was calculated from the starting monomer volume fractions Φ accounting for the density changes in the course of polymerization; $\Phi_p = \Phi\rho_m/(\Phi\rho_m + (1 - \Phi)\rho_n)$.

The polymer conversion was not included in the calculation since it was found to be negligible at higher polymer concentrations ($\Phi_p > 0.1$). One notes that $c_n(\Phi_p)$, except for low values of λ, is only weakly λ-dependent. The most pronounced λ dependence of $c_n(\Phi_p)$ is seen with low Φ_p values. Since $c_n(\Phi_p)$ should smoothly approach zero as $\Phi_p \to 0$, predictions with higher λ values seem to best describe the essential features of $c_n(\Phi_p)$.

The speed of sound in the network c_n can be used for the evaluation of the real part of the dynamic longitudinal modulus of the network, M ($=K + (4/3)G$), where K and G are the frequency-dependent compression and shear moduli, respectively) using the well-known relationship $c = (M/\rho)^{1/2}$. Values of M calculated from c_n (Table I) are plotted as a function of Φ_p in Figure 6. It is seen in this figure that M follows a power law $M \sim \Phi_p^{2.6}$ at low volume fractions ($0.1 \le \Phi_p < 0.5$) and increases faster at higher

Table II
Bulk Properties of Toluene and PMMA at Room Temperature

parameter	values	ref	parameter	values	ref
ρ_f, kg m^{-3}	866	18	n	1.49	18
ρ_n, kg m^{-3}	1190	18	$(4/3)\eta_s + \eta_B$, kg m^{-1} s^{-1}	3.8×10^{-3}	
c_0, m s^{-1}	1390				

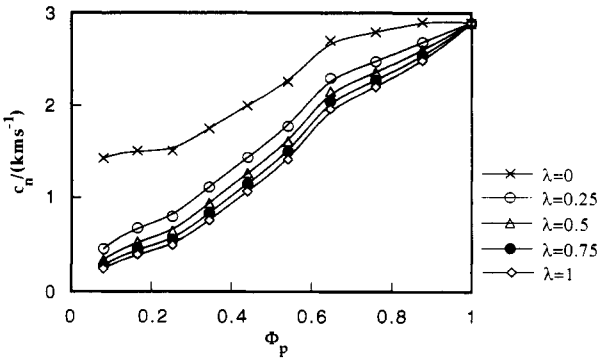

Figure 5. Φ_p dependence of the speed of sound in the polymer network, c_n, as obtained from the data in Figure 3 for the coupling parameters λ = 0–1 as indicated.

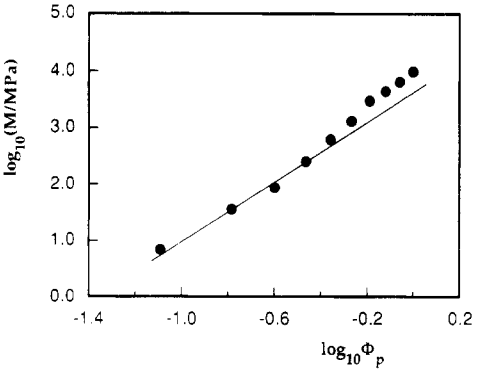

Figure 6. log–log plot of the longitudinal modulus determined from the Brillouin experiments (M) versus the polymer volume fraction (Φ_p).

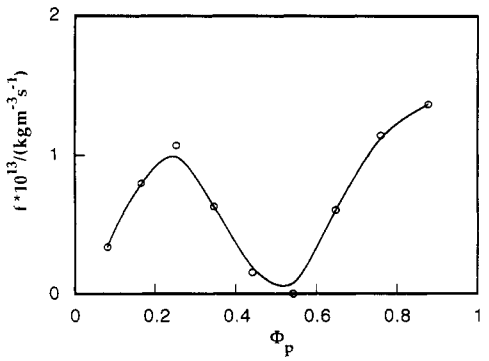

Figure 7. Friction coefficient, f, obtained from eq 2 choosing the function $c_n(\Phi_p)$ for $\lambda = 1$, as a function of Φ_p.

values of Φ_p. We note that a similar power law dependence with an exponent 2.6 was found at 333 K for polystyrene gels swollen in cyclohexane in the concentration range $0.1 \leq \Phi_p \leq 0.3$.[19] This exponent is, however, higher than the value (2.25) predicted by the blob theory.[17] The above correspondence of the M and M_{OS} behavior provides indirect evidence that this applied procedure gives a realistic description of the concentration dependences of c_n and M when the system is far from the glass transition at low polymer concentrations.

In agreement with the approach used for $c_n(\Phi_p)$, we can also estimate the friction factor f as a function of Φ_p from eq 2 choosing the function $c_n(\Phi_p)$ for $\lambda = 1$. The $f(\Phi_p)$ dependence is shown in Figure 7. Such f values are too small to satisfy the criterion of a strong frictional damping limit ($f \gg [(4/3)\eta_S + \eta_B]q^2$ or $2\pi\Delta\nu_B\rho_f(1 - \Phi_p)$) over the whole concentration region; $[(4/3)\eta_s + \eta_B]q^2 = 4.3 \times 10^{12}$ kg m^{-3} s^{-1}. This value is higher than the f values in the vicinity of the $\Delta\nu_B$ maximum (cf. Figure 7). Moreover, the minimum in f found at $\Phi_p = 0.5$ is unexpected and difficult to understand. It would seem that the applied theory breaks down in this region because the other dissipative mechanism manifests itself in this concentration region. The Marqusee and Deutch theory for gels has been used here as a possible platform to present and discuss the experimental data. Potentially, it has severe drawbacks, however. As pointed out by Patterson,[22] a weak point in the analysis is that the elastic modulus of the entanglement network of the polymer is always much too small relative to the modulus of compression to give a measurable effect on the total longitudinal modulus. Furthermore, entangled solutions are viscoelastic media and the longitudinal modulus is strongly frequency dependent. All these effects are ignored in the theory. Nevertheless, the theory is able to provide a realistic description of the modulus in the concentration range $0.1 < \Phi_p < 0.5$ and for the friction coefficient in the range $\Phi_p = 0.1$–0.3.

Despite the realistic description of the concentration dependence of the modulus M, a major discrepancy originates in the elasticity of concentrated solutions. Quasielastic light scattering measurements made at $\Phi_p = 0.1$ suggest that the low-frequency value $M_{os} = 3.9$ MPa is more than an order of magnitude smaller than the value determined using Brillouin measurements. Similarly, the friction coefficient f from Brillouin measurements is lower by an order of magnitude than that calculated for semidilute solutions employing the solvent viscosity ($f = 4.7 \times 10^{14}$ kg m^{-3} s^{-1}). A similar discrepancy was found in the sound absorption measurements of Bacri et al.[20] A plausible explanation for these differences, retaining the current theoretical framework, is the possibility of dispersion in both the elasticity of the network and the friction coefficient.

Conclusions

We have carried out an experimental study of the Brillouin spectra of a binary system consisting of poly(methyl methacrylate) and toluene mixtures at various polymer concentrations and temperatures. It is shown that the temperature dependences of the Brillouin frequency and line width are very similar to those observed previously in polystyrene/cyclohexane solutions.[9] We also discuss the concentration dependences of the Brillouin frequency and line width in terms of a theory for Brillouin light scattering from gels proposed by Marqusee and Deutch.[14] It is shown that the theoretical equations in the limit of strong frictional damping and strong coupling between sound waves in the fluid and elastic waves in the polymer network can be adopted to analyze the experimental results. The speed of sound in the network, longitudinal modulus, and frictional damping have been evaluated from the Brillouin frequency and line width, respectively. The Marqusee and Deutch theory provides a realistic description in the lower concentration ranges but breaks down in the vicinity of the Brillouin line-width maximum ($\nu_B \approx 1/\tau_s$) and gives values of the frictional coefficient which are too small in this region.

A more extensive discussion of the concentration dependences of the longitudinal modulus, M, evaluated from the Brillouin frequency shifts and the osmotic modulus, M_{os}, from the static and quasielastic light scattering experiments will be given in conjunction with the presentation of results for the polystyrene/toluene and poly(butyl acrylate) systems in forthcoming papers.

Acknowledgment. This work has been supported by the Swedish Natural Science Research Council (NFR) and the Swedish Board for Technical Development (STU). We thank Professor G. D. Patterson for constructive comments.

References and Notes

(1) Patterson, G. D. *Molecular Structure and Dynamics*; Fara, R., Ed.; Academic Press: New York, 1980.
(2) Wendorff, J. H. *Prog. Colloid Polym. Sci.* **1979**, *66*, 183.
(3) Tanaka, T.; Hocker, L. O.; Benedek, G. B. *J. Chem. Phys.* **1973**, *59*, 5151.
(4) Stepanek, P.; Konak, C. *Adv. Colloid Interface Sci.* **1984**, *21*, 195.
(5) Brown, W.; Nicolai, T. *Prog. Colloid Polym. Sci.* **1990**, *268*, 977.
(6) Bedborough, D. S.; Jackson, D. A. *Polymer* **1976**, *17*, 573.
(7) Lindsay, S. M.; Shepherd, I. W. *Probing Polymer Structures*; Koening, J., Ed.; American Chemical Society: Washington, DC, 1979.
(8) Adshead, A.; Lindsay, S. M. *Polymer* **1980**, *21*, 1355.
(9) Lempert, W.; Wang, C. H. *J. Chem. Phys.* **1980**, *72*, 2570.
(10) Jarry, J. P.; Patterson, G. D. *Macromolecules* **1981**, *14*, 1281.
(11) Adshead, A.; Lindsay, S. M. *Polymer* **1982**, *23*, 1884.
(12) Ng, S. C.; Hosea, T. J. C.; Gan, L. M. *J. Phys. Lett.* **1985**, *46*, L887.
(13) Konak, C.; Pavel, M.; Dusek, K. *Polym. Bull.* **1989**, *21*, 641.
(14) Marqusee, J. A.; Deutch, J. M. *J. Chem. Phys.* **1981**, *75*, 5239.
(15) Marquardt, D. W. *J. Soc. Ind. Appl. Math.* **1963**, *11*, 431.
(16) Press, W. H.; Flannery, B. P.; Teukolsky, S. A.; Vetterling, W. T. *Numerical Recipes: The Art of Scientific Computing*; Cambridge University Press: Cambridge, U.K., 1988.
(17) de Gennes, P.-G. *Scaling Concepts in Polymer Physics*; Cornell University Press: Ithaca, NY, 1979.
(18) *Polymer Handbook*; Brandrup, J., Immergut, E. H., Eds.; John Wiley and Sons: New York, 1967.
(19) Davidson, N. S.; Richards, R. W.; Geissler, E. *Polymer* **1985**, *26*, 1643.
(20) (a) Bacri, J. C.; Courdille, J. M.; Dunas, J.; Rajaonarison, R.; *J. Phys., Lett.* **1980**, *41*, 372. (b) Bacri, J. C.; Rajaonarison, R. *J. Phys. Lett.* **1978**, *40*, 5.
(21) Floudas, G.; Fytas, G.; Brown, W. *J. Chem. Phys.*, in press.
(22) Patterson, G. D., personal communication.

Registry No. PMMA (homopolymer), 9011-14-7; PhMe, 108-88-3.